

IFSCC 2025 full paper (IFSCC2025-141)

Senescence of Dermal Fibroblasts Contributes to the Formation of Solar Lentigo: Functional Analysis of a Novel Anti-Hyperpigmentation Factor sFRP1

Daiki Yamakoshi¹, Yuri Sato¹, Chen Jiaxu¹, Hiroe Ochi¹, Yuki Ito¹, Alan B. Fleischer², Viki Swope², Renny Starner², Toru Atsugi¹, Yuki Mizutani¹, Zalfa A. Abdel-Malek²

¹ Research Laboratories, KOSÉ Corporation, Tokyo, Japan

² Department of Dermatology, University of Cincinnati, Cincinnati, Ohio, United States

1. Introduction

Skin aging has long been a subject of interest in dermatology and cosmetology, with solar lentigo (SL) being one of the most common concerns among people in their 30s and older. SL is a type of hyperpigmentation that primarily develops due to chronic ultraviolet (UV) exposure and aging, leading to the abnormal accumulation of melanin in the epidermis. Previous studies have mainly focused on the regulation of melanogenesis in melanocytes and the differentiation of epidermal cells as key mechanisms in SL formation. Nevertheless, clinical findings indicate that even after interventions targeting the epidermis such as laser treatment, SL occasionally recurs at the same location with a similar shape. Moreover, anti-pigmentary cosmetic solutions targeting keratinocytes and melanocytes have not been globally effective for treatment of SL lesions.

Recent studies have provided evidence supporting the involvement of dermal components in SL development. Duval et al. reported that skin models containing senescence-induced fibroblasts exhibited enhanced melanin accumulation in the epidermis, suggesting that the secretome of senescent fibroblasts contributes to hyperpigmentation [2]. Unlike the epidermis, the dermis has a much slower turnover rate, making it more prone to accumulating aging-related damage. These findings suggest that the dermal aging may play a significant role in the formation and progression of SL, and highlight the dermis as a novel therapeutic target for hyperpigmentation.

However, the specific mechanisms by which dermal aging contribute to SL formation remain largely unexplored. Most previous transcriptomic studies on SL have analyzed RNA from full-thickness skin samples [3-5]. Consequently, these studies have mainly captured gene expression changes in the epidermis, potentially overlooking critical alterations occurring in the dermis. A major challenge in addressing this gap is the inherently low cellular density of the dermis, which makes it difficult to analyze dermis-specific changes. To overcome this limitation, it is necessary to separate the epidermis and dermis and analyze each layer independently.

The aim of this study was to elucidate the role of dermal aging in the development of SL and to explore novel therapeutic strategies targeting dermal factors. We performed transcriptomic analysis of dermis-specific RNA isolated from enzymatically separated skin biopsies. This approach identified Secreted Frizzled-Related Protein 1 (sFRP1), a WNT signaling regulator, as significantly downregulated in the dermis of SL lesions. sFRP1 expression was downregulated in senescent fibroblasts. Functional studies using cultured melanocytes and 3D skin models demonstrated that sFRP1 suppresses melanogenesis. Furthermore, we identified a plant extract that enhances sFRP1 production in cultured fibroblasts, and that conditioned media of fibroblasts pre-treated with the extract reduce epidermal pigmentation. These findings indicate that age-related downregulation of sFRP1 in the dermis plays a critical role in SL development and propose sFRP1 upregulation as a promising well-aging strategy for the management of hyperpigmentation.

2. Materials and Methods

2.1. Biopsy collection

Eight female Caucasian subjects with Fitzpatrick skin type I or II and ranging in age between 57-68 (mean 62 years) were enrolled. All volunteers underwent a skin examination conducted by the dermatologist to diagnose SL. Informed written consent was obtained from subjects before skin biopsy, and this study was approved by the University of Cincinnati Institutional Review Board (ID: CR02_2019-0473). Two 5 mm shave biopsies were obtained, one from an SL lesion and one from adjacent perilesional normal skin.

2.2. Gene expression analysis

The epidermis and dermis were isolated from the collected skin biopsies using Dispase II (Roche), and total RNA was extracted from each compartment for RNA-seq and qRT-PCR analysis. The data of RNA-seq were visualized using MA-plots to identify genes with significant expression changes in the dermis of SL compared to normal skin.

2.3. Sample collection from skin cell cultures

Cultured human melanocytes, fibroblasts, and keratinocytes were harvested 96 hours after seeding, and total proteins were isolated for Western blotting. Culture supernatants were also collected at the same time point for ELISA analysis. For each cell type, 3 different cell cultures were used.

2.4. Induction of senescent fibroblasts

Primary human dermal fibroblasts were induced to undergo cellular senescence via two different methods: (I) replicative senescence, achieved through continuous passaging until proliferative capacity was exhausted, and (II) oxidative stress-induced senescence, achieved by treating the cells with hydrogen peroxide (H_2O_2) at concentrations of up to 600 μM for 2 hours.

2.5. Primary human melanocyte cultures

Primary human melanocyte cultures were established from 3 different neonatal foreskins and used for the experiments hereby described. All cultures were maintained under identical conditions as described previously [6]. Cultured melanocytes were treated with sFRP1 recombinant protein (rsFRP1, Sigma-Aldrich) at concentrations of 0.1 $\mu g/mL$ or 1 $\mu g/mL$. The fresh

medium and treatment were added every other day for a total of 4 days or 6 days. Tyrosinase activity was assayed as described previously [7]. Protein levels of cyclin D1, tyrosinase and β -catenin were tested by Western blotting.

2.6. 3D skin model cultures

3D cultured human epidermal skin models were purchased from Mattek Corporation (MEL-300B). The fresh medium and rsFRP1 were added every other day. After 12 days, the cultured skin samples were fixed in 4% PFA, embedded in OCT and cryo-sectioned. Sections were subjected to Fontana-Masson staining for melanin visualization and immunofluorescence staining using antibodies for β -catenin (Santa Cruz Biotechnology) and TYRP1 (Atlas antibodies). The models were removed from the culture inserts and total melanin was extracted and quantified spectrophotometrically with absorbance at 405 nm.

2.7. Treatment of fibroblasts with plant extract

Green rooibos (*Aspalathus linearis*) extract was applied to cultured fibroblasts at concentrations of up to 1.85 μ g/mL for 24 hours. The conditioned media collected from the treated fibroblasts was mixed with melanocyte culture medium at a 1:3 ratio, and melanocytes were cultured in this medium. Tyrosinase activity was measured 72 hours after treatment.

2.8. qRT-PCR analysis

The total RNA from each sample was converted into cDNA. The sequences of the primers used in this study are as follows:

sFRP1: 5'-CCAGCGAGTACGACTACGTGAGCTT-3', 5'-CTCAGATTCAACTCGTTGTCACAGG-3', GAPDH: 5'-CTGACTTCAACAGCGACACC-3', 5'-TGCTGTAGCCAAATTCGTTG-3'.

2.9. Western blotting

Antibodies specific for sFRP1 (Abcam), cyclin D1 (Abcam), tyrosinase (Santa Cruz Biotechnology), β -catenin (Santa Cruz Biotechnology), and GAPDH (Abcam) were used as the primary antibodies. Rabbit IgG horseradish peroxidase (HRP)-linked whole antibody (GE Healthcare, for sFRP1 and cyclin D1) and mouse IgG HRP-linked whole antibody (GE Healthcare, for tyrosinase, β -catenin and GAPDH) were used as the secondary antibodies. Densitometry analysis was conducted, comparing each band to its respective GAPDH loading control.

2.10. ELISA

The concentration of secreted sFRP1 in the conditioned culture media was measured using sFRP1 ELISA kits (Abcam), following the manufacturer's instructions. Each data point was normalized to cell number.

2.11 Statistical analysis

Statistical analyses were performed using JMP software (SAS). Data are expressed as the mean \pm standard error of the mean from at least three samples. Statistical significance was determined using Welch's t-test, one-way ANOVA followed by Tukey's HSD or Dunnett's test. A p-value <0.05 was considered statistically significant.

3. Results

3.1. Gene analysis of solar lentigo

Skin biopsies from SL lesions and non-lesional sun exposed skin areas were separated into the epidermis and dermis, and total RNA was extracted from each layer (Fig. 1A). Genes with high expression levels (\log_{10} average expression > 3) and large expression changes (\log_2 relative expression > 2 or < -2) were defined as biologically significant differentially expressed genes (Fig. 1B). Candidate genes were further selected according to two criteria: (I) expression of features characteristic of secreted proteins, and (II) potential involvement in biological pathways related to melanogenesis. As a result, sFRP1, a known regulator of the WNT signaling pathway, was identified as being downregulated in the SL region. sFRP1 is a member of the sFRP gene family and is known to bind to WNT ligands, thereby inhibiting WNT signaling. To further investigate sFRP1 expression changes, epidermal and dermal RNA from 8 donors was analyzed. The results showed no significant changes in sFRP1 expression in the epidermis, while 75% of donors (i.e. 6/8 subjects) exhibited a reduction in sFRP1 expression in the dermis, with an average decrease of 43% in SL, as compared to NL (Fig. 1C).

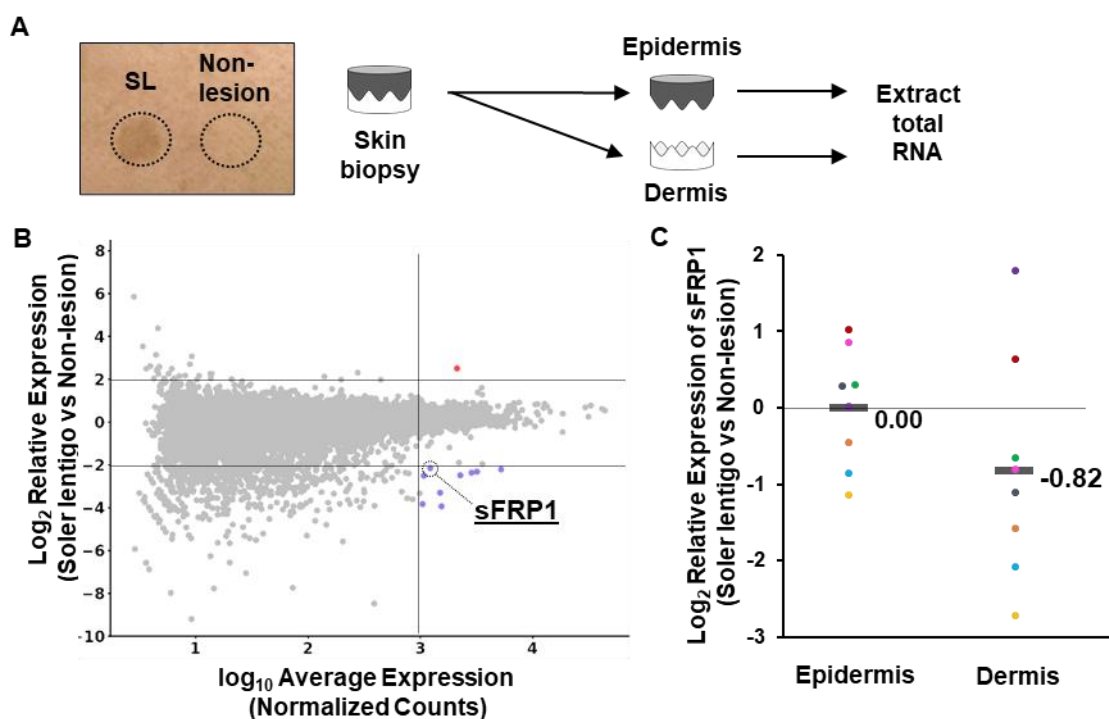


Figure 1. Gene expression analysis in the dermis of solar lentigo

(A) Skin biopsies were taken from SL and adjacent non-lesional (NL) areas. The epidermis and dermis were separated, and total RNA was extracted from each layer. (B) The \log_2 fold change values of dermal gene expression in SL relative to NL are plotted against the \log_{10} average normalized counts ($N=2$ donors). Each point represents a gene. Genes with $\log_2\text{FC} > 2$ or < -2 and a \log_{10} average > 3 are considered biologically significant and are highlighted in red (upregulated) or blue (downregulated). (C) The \log_2 fold change values of sFRP1 expression in SL relative to the NL are plotted. Individual data points, represented by different colors, correspond to measurements from individual donors ($N=8$). The black bars and the numbers indicate the mean values.

3.2. sFRP1 expression analysis in skin cells

To further identify the skin cell types responsible for sFRP1 production and secretion, sFRP1 expression levels were analyzed in primary cultures of key skin cell types, including keratinocytes, melanocytes, and fibroblasts. For each cell type, experiments were performed using 3 different cell cultures. Among these cell types, fibroblasts exhibited the highest sFRP1 expression. Keratinocytes also expressed sFRP1, whereas no detectable expression was observed in melanocytes. Consistent results were obtained in Western blotting and ELISA (Fig. 2).

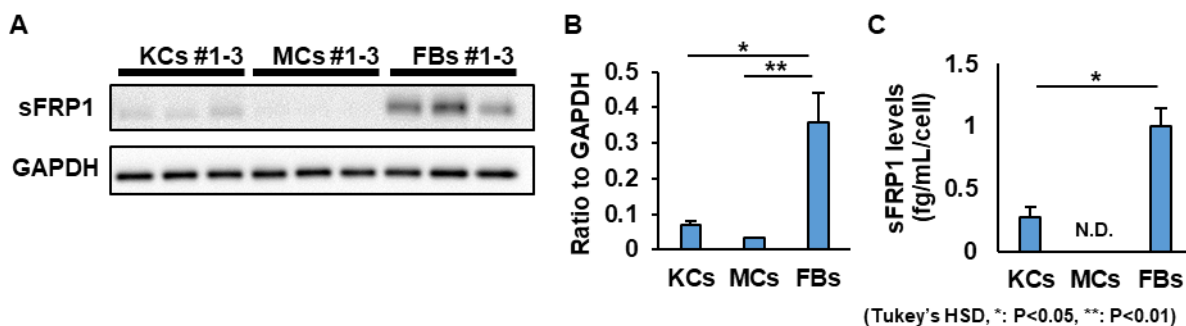


Figure 2. sFRP1 expression in different human skin cell types

(A, B) sFRP1 expression levels in keratinocytes (KCs), melanocytes (MCs), and fibroblasts (FBs) were measured by Western blotting. GAPDH was used as a loading control. (C) sFRP1 protein levels in culture supernatants of KCs, MCs, and FBs as determined by ELISA.

3.3. Influence of cellular senescence on sFRP1 expression in fibroblasts

Previous studies have reported that senescent fibroblasts accumulate in the dermis of SL [8]. Here, we induced cellular senescence in fibroblasts using replicative senescence and oxidative stress and analyzed the effects on sFRP1 expression. sFRP1 expression was significantly downregulated in both senescent models ($n=3$; Fig. 3).

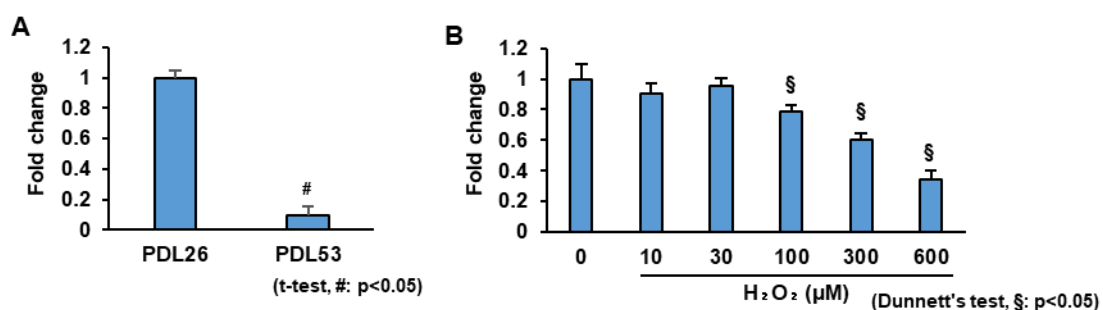


Figure 3. Expression changes of sFRP1 in senescent fibroblasts

sFRP1 expression levels were analyzed using qRT-PCR in cultured fibroblasts under different senescence-inducing conditions. (A) Replicative senescence: PDL26 and PDL53 correspond to the non-senescent and senescent stages, respectively. (B) Oxidative stress-induced senescence: The fibroblasts treated with hydrogen peroxide (H_2O_2) for 2 hours at the concentrations indicated in the graph. The cells were harvested 24 hours after the treatment and the total RNA was extracted.

3.4. Effects of sFRP1 on cultured melanocytes

To examine the biological effects of sFRP1 secreted by other cell types on melanocytes, rsFRP1 was added to the culture medium of melanocytes at concentrations of 0.1 µg/mL or 1 µg/mL, with fresh media and treatment added every other day.

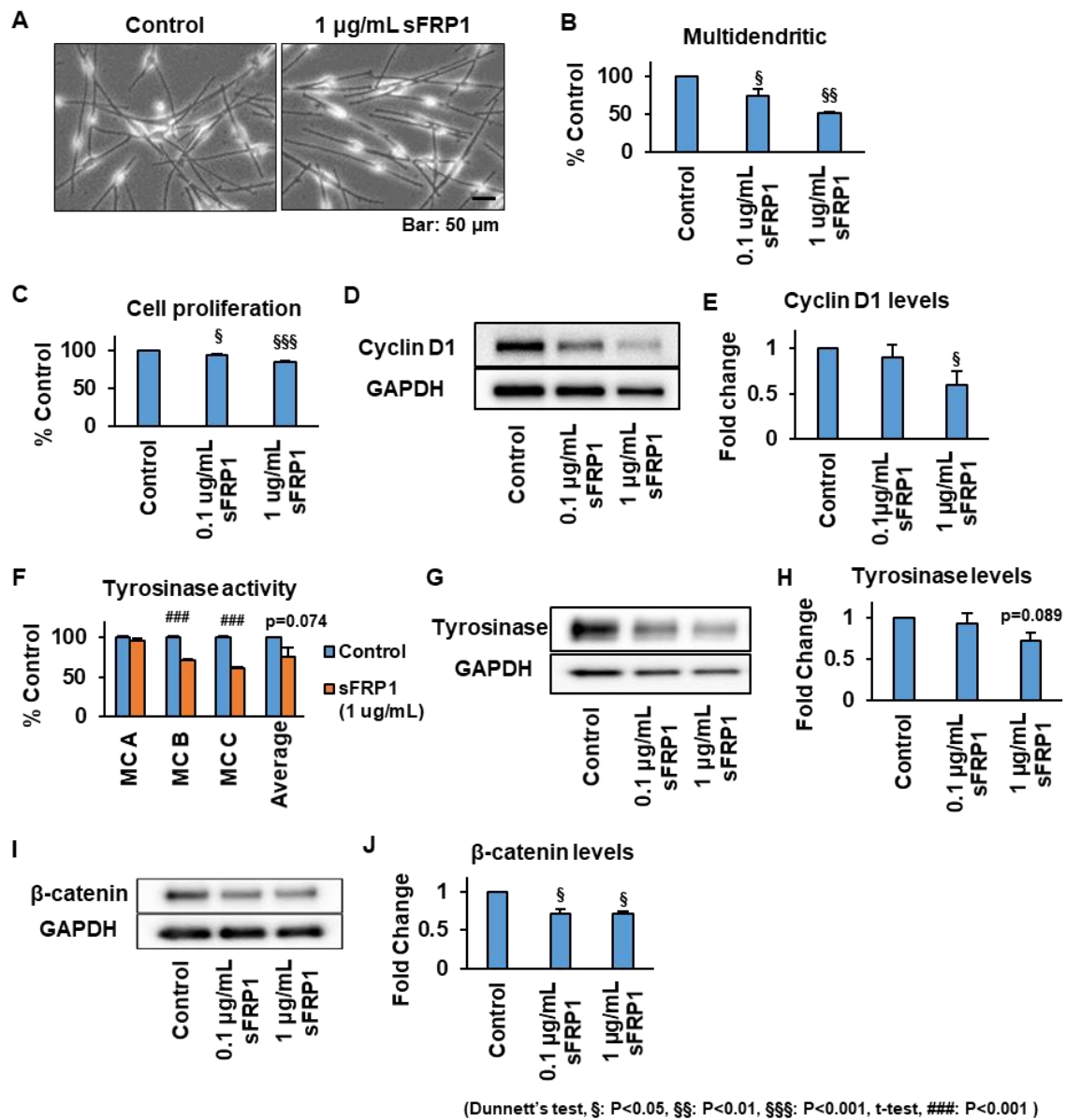


Figure 4. Effects of sFRP1 on cultured melanocytes

Human normal melanocytes from 3 different donors were cultured for 4–6 days in medium containing rsFRP1. (A) Representative images of the morphology of the melanocytes after 4 days treatment are shown. (B) The ratio of cells with three or more dendrites was quantified. (C) Cell number was counted after 4 days treatment. (D, E) Protein expression levels of cyclin D1 were assessed by Western blotting after 4 days treatment. (F) Tyrosinase activity was determined after 6 days of treatment, normalized to cell number then expressed as % of untreated control. (G–J) Protein expression levels of tyrosinase and β-catenin were assessed by Western blotting after 4 days treatment.

After four days of treatment, the morphologies of cells with three or more dendrites were quantified and their ratio relative to total number of melanocytes was significantly reduced in the sFRP1-treated group (Fig. 4A, B). The cell number of melanocytes also decreased by sFRP1 treatment (Fig. 4C). Furthermore, Western blotting revealed that the expression of cyclin D1, a positive regulator of the G1-to-G2 transition, was significantly reduced in the group treated with 1 µg/mL sFRP1 (Fig. 4D, E). To evaluate the effect on melanogenesis, tyrosinase activity and expression levels were tested. Results showed that tyrosinase activity was inhibited by the sFRP1 treatment in two out of the three donors (Fig. 4F), and Western blot analysis showed a trend toward decreased tyrosinase expression ($p=0.089$ by Dunnett's test, Fig. 4G, H). Western blot analysis of β -catenin, a key component upregulated during WNT signaling activation, showed a significant reduction in the sFRP1-treated group (Fig. 4I, J).

3.5. Effects of sFRP1 on 3D skin models

To investigate the role of sFRP1 in pigmentation, 3D epidermal skin models containing melanocytes were cultured in media supplemented with rsFRP1 protein. Fontana-Masson staining showed that pigmentation was reduced in the sFRP1-treated group (Fig. 5A). Quantification of melanin content showed that melanin levels were significantly decreased in the sFRP1-treated group ($n=3$; Fig. 5B). In addition, immunofluorescence staining revealed that rsFRP1 treatment altered the subcellular localization of β -catenin, promoting its accumulation in the cytoplasm rather than in the nucleus (control: $n=2$, 1 µg/mL sFRP1: $n=3$; Fig. 5C, D).

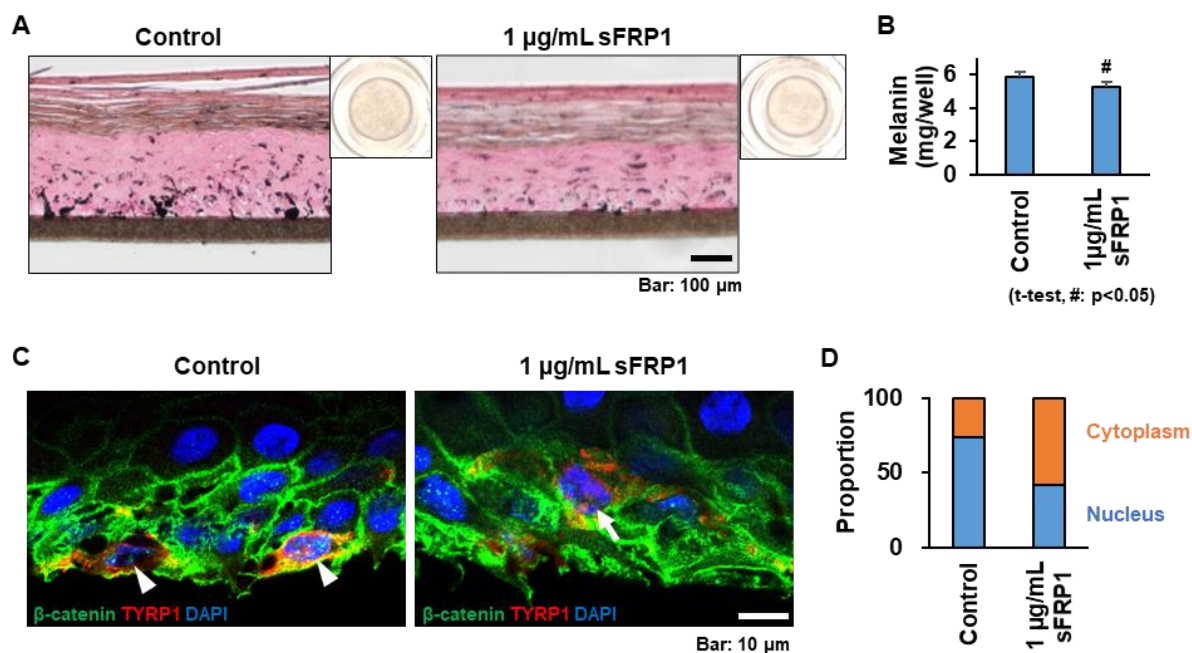


Figure 5. Effects of sFRP1 on 3D skin models

(A) Histological sections of 3D skin models were stained with Fontana-Masson, and inserts display the appearance of the skin models. (B) Melanin content per well was quantitatively analyzed. (C) Representative immunofluorescence images show β -catenin (green), nuclei (blue, stained with DAPI), and TYRP1 (red, a melanocyte marker). Arrowheads indicate the localization of β -catenin at the nuclei in melanocytes, and the arrow indicates its absence from the nuclei. (D) The proportion of β -catenin localized in the nucleus and cytoplasm was quantified and the mean values are shown.

3.6. Identification of active compounds that increase sFRP1 expression

A screening of plant extracts for their ability to enhance sFRP1 expression was conducted. This revealed that green rooibos extract, which is derived from unfermented rooibos leaves and is rich in polyphenols with strong antioxidant properties, increased sFRP1 expression by 25% in fibroblasts upon treatment with 1.85 µg/mL extract ($n=3$; Fig. 6A). The conditioned medium of fibroblasts treated with green rooibos extract decreased tyrosinase activity by 20% in cultured melanocytes ($n=3$; Fig. 6B).

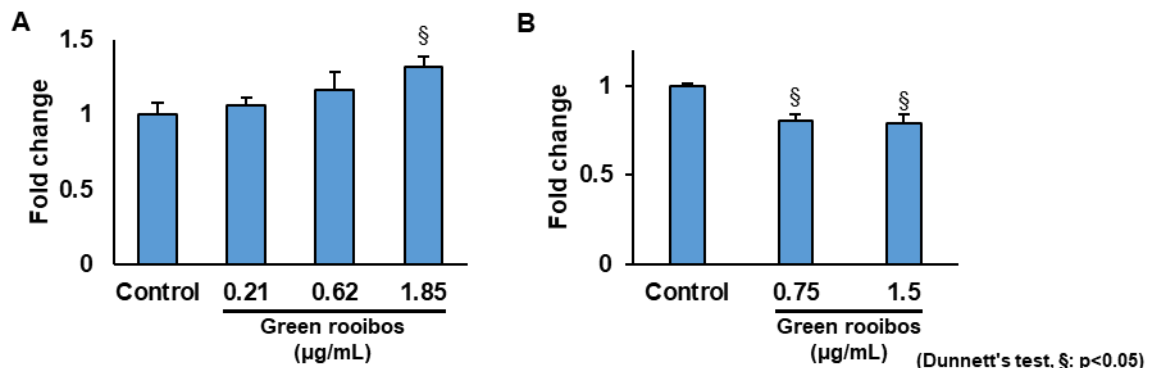


Figure 6. Green rooibos extract increases sFRP1 expression in fibroblasts and reduces melanogenic activity in melanocytes

(A) Screening of various plant extracts identified green rooibos (*Aspalathus linearis*) extract as a potent inducer of sFRP1 expression in cultured human dermal fibroblasts. Cells were treated with increasing concentrations of green rooibos extract, and sFRP1 mRNA expression was quantified by qPCR. (B) Melanocytes were treated with conditioned medium derived from fibroblasts pre-treated with green rooibos extract. Tyrosinase activity was measured by tyrosinase assay.

4. Discussion

It has long been established that melanocyte function and homeostasis are regulated by a plethora of paracrine factors produced by adjacent epidermal keratinocytes. Subsequent studies have revealed that dermal fibroblasts, in addition to keratinocytes, also synthesize factors that regulate melanogenesis [9]. Recent studies have further suggested that fibroblast senescence contributes to pigmentary disorders such as SL [2]. However, the specific changes occurring in the dermis of SL lesions and the molecular mechanisms by which these changes promote hyperpigmentation have remained unclear.

In this study, we aimed to clarify the involvement of dermal aging in the pathogenesis of SL and we revealed that the expression of sFRP1, a modulator of the WNT signaling pathway, was significantly downregulated in SL. In contrast, no marked changes in sFRP1 expression were observed in the epidermis. This finding suggests that previous transcriptomic analyses, which assessed full-thickness skin may have overlooked dermis-specific changes. By isolating and analyzing dermal RNA separately, we successfully identified the specific downregulation of sFRP1 in the dermis of SL.

WNT signaling promotes melanogenesis by inducing β-catenin nuclear translocation. In the canonical pathway, sFRP1 binds to WNT ligands, preventing their interaction with WNT receptors, thereby inhibiting β-catenin stabilization and WNT signaling activation in melanocytes and reducing melanogenesis. However, Kim et al. reported that sFRP2, another member of the sFRP family, directly interacts with WNT receptors in melanocytes and enhances melanogenesis [10]. These findings demonstrate that the regulation of WNT signaling by sFRP family

members is highly dynamic and varies depending on the specific sFRP. To investigate the role of sFRP1 on melanocytes, we conducted functional analyses using recombinant sFRP1 protein in cultured melanocytes. Interestingly, unlike sFRP2, we found that sFRP1 suppressed melanocyte proliferation, dendrite formation, and melanogenesis (i.e. tyrosinase activation and expression). sFRP1 reduced β -catenin levels in melanocytes, suggesting that sFRP1 inhibits WNT signaling and thereby suppresses melanocyte activity. Furthermore, experiments using a 3D skin model showed a significant reduction in melanin content, indicating that sFRP1 functions as a suppressor of epidermal pigmentation. In addition, immunofluorescence analysis revealed decreased nuclear localization of β -catenin in melanocytes by sFRP1 treatment, suggesting that inhibition of the WNT signaling pathway also occurred within the 3D skin models.

Analysis of sFRP1 expression in major skin cell types revealed that sFRP1 is primarily secreted by fibroblasts in skin and likely acts on melanocytes in a paracrine manner. Previous studies reported that senescent fibroblasts accumulate in the dermis of hyperpigmented skin [8]. In this study, we confirmed that sFRP1 production was reduced in fibroblasts undergoing replicative senescence or oxidative stress-induced senescence. Liang et al. reported that chronic UV exposure promotes DNA methylation, leading to decreased expression of sFRP1 in keratinocytes [11], suggesting that a similar epigenetic mechanism may occur in dermal fibroblasts. Based on these findings, we postulate that fibroblast senescence leads to decreased sFRP1 expression and subsequent dysregulation of pigmentation.

Collectively, our results demonstrate that sFRP1 plays a key role in maintaining skin homeostasis. The decline in sFRP1 function, due to fibroblast senescence, leads to increased melanin accumulation in the epidermis, contributing to the formation and exacerbation of hyperpigmentation. Our proposed model is shown in Fig. 7.

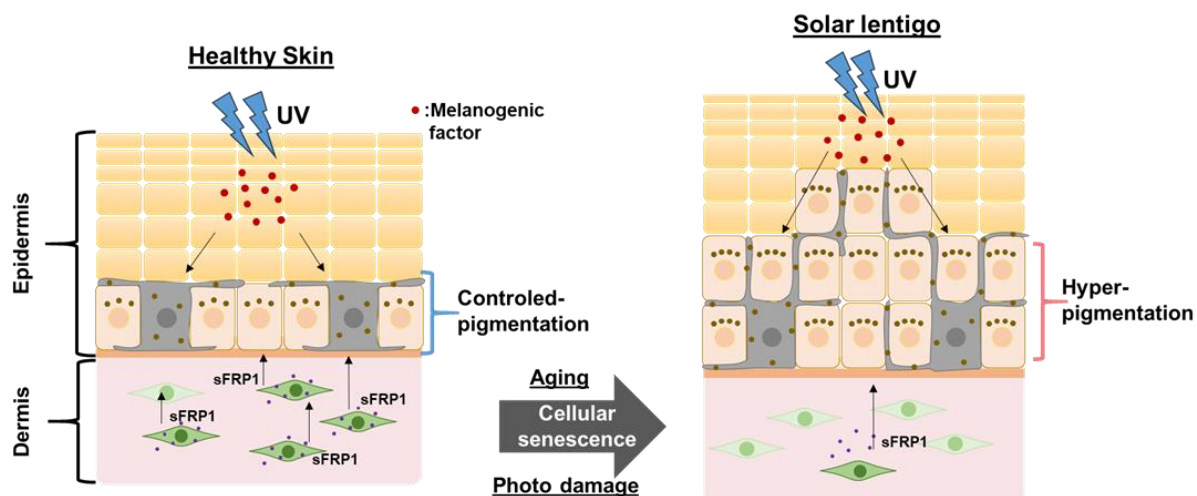


Figure 7. Proposed model of solar lentigo development involving sFRP1

In normal young skin (left), dermal fibroblasts secrete sFRP1, which helps maintain balanced melanocyte activity and melanin distribution in the basal layer of the epidermis, even under UV exposure. In solar lentigo (right), senescent fibroblasts show decreased secretion of sFRP1, which allows for increased melanogenesis.

Conventional treatments for hyperpigmentation have largely focused on inhibiting melanin synthesis or promoting melanin degradation. Our study proposes a novel therapeutic strategy that targets dermal aging by enhancing the production of sFRP1, an endogenous anti-hyperpigmentation factor inherently present in the dermis. We identified green rooibos extract as an agent capable of upregulating sFRP1 expression in fibroblasts and reducing tyrosinase activity in melanocytes, suggesting its potential application in cosmetics and functional food products for treating hyperpigmentation. Advances in tissue rejuvenation technologies may further accelerate the development of this strategy [12], particularly for SL. This approach not only complements existing therapies but also offers a more fundamental and sustained solution for pigmentation disorders.

5. Conclusion

Our findings highlight the importance of preserving and enhancing the skin's innate protective mechanisms to prevent pigmentation abnormalities. Targeting dermal aging by sustaining endogenous factors like sFRP1 offers a fundamental strategy for achieving well-aging through the maintenance of skin homeostasis.

6. References

1. Arora P, Sarkar R, Garg VK, Arya L., J Cutan Aesthet Surg. 2012;5(2):93–103.
2. Duval C, Cohen C, Chagnoleau C, Flouret V, Boury C, Bernerd F., PLoS One. 2014;9(12):e114182.
3. Aoki H, Moro O, Tagami H, Kishimoto J., Br J Dermatol. 2007;156(6):1214–23.
4. Warrick E, Duval C, Nouveau S, Navratil V, Vincent S, Pinel-Marie ML, *et al.*, Br J Dermatol. 2017;177(6):1619–32.
5. Choi W, Yin L, Smuda C, Batzer J, Hearing VJ, Kolbe L., Exp Dermatol. 2017;26(3):242–8
6. Abdel-Malek ZA, Swope VB, Suzuki I, Akcali C, Harriger MD, Boyce ST, *et al.*, Proc Natl Acad Sci USA. 1995;92(5):1789–93.
7. Abdel-Malek ZA, Swope VB, Pallas J, Krug K, Nordlund JJ., J Cell Physiol. 1992;150(2):416–25.
8. Yoon JE, Kim Y, Kwon S, Kim M, Kim YH, Kim JH, *et al.*, Theranostics. 2018;8(17):4620–32.
9. Gao X, Xiang W., J Cosmet Dermatol. 2025;24(1):e16790.
10. Kim M, Han JH, Kim JH, Park TJ, Kang HY., J Invest Dermatol. 2016;136(1):236–44.
11. Liang J, Liu L, Tang H, Ma Q, Sang Y, Kang X., Exp Dermatol. 2022;31(9):1443–53.
12. Dutra Alves NS, Reigado GR, Santos M, Caldeira IDS, Hernandes HDS, Freitas-Marchi BL, *et al.*, Front Bioeng Biotechnol. 2025;13:1527854.